NUMERICAL SIMULATION OF NONLINEAR VIBRATION RESPONSE OF A CYLINDRICAL WATER STORAGE TANK BY EXPLICIT FINITE ELEMENT METHOD

Akira MAEKAWA
Institute of Nuclear Safety System, Inc.,
64 Sata, Mihama-cho, Mikata-gun, Fukui 919-1205, Japan

Katsuhisa FUJITA
Institute of Nuclear Safety System, Inc. and Osaka City University,
64 Sata, Mihama-cho, Mikata-gun, Fukui 919-1205, Japan

Hiroshi OGAWA
Kawasaki Plant Systems, Ltd.,
11-1, Minamisuna, 2-chome, Koto-ku, Tokyo 136-8588, Japan

ABSTRACT

The seismic design of thin cylindrical water storage tanks takes into account beam-type vibration but not simultaneous oval-type vibration. In this study, an experimental and analytical investigation was conducted on the nonlinear response of beam-type vibration upon the generation and growth of oval-type vibration. The resonance frequency of the beam-type vibration shifted to a lower region and the magnification factor decreased with the increase in oval-type vibration by large input excitation. The application of a nonlinear single-degree-of-freedom system model revealed that this response was due to coupling between the beam-type vibration and oval-type vibration. In addition, a nonlinear finite element method capable of accurately simulating oval-type vibration is proposed. The new method simulates the nonlinear response of beam-type vibration with a high degree of accuracy.

1. INTRODUCTION

The walls of large-scale cylindrical water storage tanks are thin and deformable. These walls, together with the water contained in the tank, create a coupling vibration system between the fluid and the structure in which beam-type or oval-type vibration occurs. Clarification of the coupling vibration behavior is a significantly fundamental issue in seismic design. Considerable research has been conducted on beam-type vibration and oval-type vibration (Chiba et al., 1986; Amabili, 2000; Fujita and Saito, 2003). However, there is a little research regarding the vibration behavior caused by coupling between beam-type and oval-type vibration. Here, beam-type vibration defines vibration modes that have axial half wave number $m \geq 1$ and circumferential wave number $n = 1$. Oval-type vibration defines higher-order vibration modes in the circumferential direction and generated on the sidewall, with $m \geq 1$ and $n \geq 2$. Both oval-type and beam-type vibration simultaneously occur during earthquakes. Therefore, it is necessary to clarify the influence of oval-type vibration on beam-type vibration, the behavior of which is a significant issue in seismic design.

In this study, sinusoidal frequency sweep tests by large input excitation were conducted using a cylindrical test tank. Then, the nonlinear response of the beam-type vibration was investigated when the oval-type vibration increased by large excitation. Next, assuming that the amplitude of oval-type vibration causes some out-of-plane deformation of the test tank sidewall and a decrease in flexural rigidity, it is proposed that the characteristics of beam-type vibration change due to coupling between beam-type and oval-type vibration. Based on the proposal, an equivalent nonlinear coupling vibration model with a single-degree-of-freedom (1DOF) system was created. It was demonstrated that this model can satisfactorily explain the results of the sweep tests. In addition, a new analysis method based on the finite element method simulating oval-type vibration is proposed. The method verified that the nonlinear response of beam-type vibration obtained in the tests occurs due to coupling between beam-type and oval-type vibration.

2. VIBRATION EXPERIMENT

2.1 Experimental method

Figure 1 shows a photo of the test tank used in the vibration experiment. Figure 2 shows the dimensions and shape of the test tank. The cylindrical part of the test tank is aluminum alloy and the top and bottom parts are fixed by steel flanges. The input acceleration applied by the shaking table and the response acceleration at the top of the tank are measured by accelerometers set on the shaking table and at the top of the tank. The response acceleration at the top represents the response acceleration of beam-type vibration. Non-contact type displacement meters, which are laser displacement sensors, are set at 0° and at a tank height of 1200 and 680 mm. Displacement at the 1200-mm height represents the displacement at the top of the test tank and the amplitude of beam-type vibration. Displacement at the 680-mm height represents that of the body of the tank and the amplitude of oval-type vibration.

Frequency sweep tests were conducted by sinusoidal excitation using the test tank 95% filled with water (1140 mm of the tank height). The bottom of the tank was excited by the shaking table between 0° and 180° horizontally. The sweep extent of excitation frequency included the primary natural frequency of beam-type vibration. The sweep rate was set at 0.2 Hz/s. A varying magnitude of input acceleration was adopted. The other test conditions are shown in Table 1. Amplitude and phase response curves were calculated using the input acceleration and response acceleration at the top and then the predominant frequency and change of magnification factor were investigated. In this paper, resonance frequency is defined as the predominant frequency.

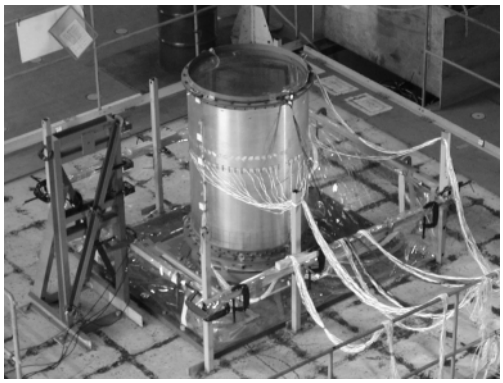

Figure 1: *Test tank.*

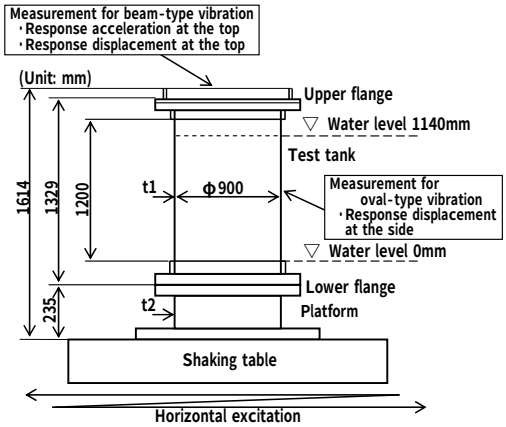

Figure 2: *Dimensions and shape of test tank.*

Case	Input acc. (G)	Exciting frequency range (Hz)
1	0.09	5 – 49.5
2	0.09	49.5 – 5
3	0.11	5 – 49.5
4	0.11	49.5 – 5
5	0.21	5 – 49.5
6	0.21	49.5 – 5
7	0.54	5 – 49.5
8	0.55	49.5 – 5
9	1.16	5 – 49.5
10	1.56	5 – 49.5
11	0.11	5 – 49.5

Table 1: *Test conditions.*

2.2 Experimental results

Figures 3 and 4 show key examples of the amplitude and phase response curves, taken from Cases 1, 7 and 9. Both figures demonstrate a nonlinear vibration response in which the resonance frequency shifts to a lower region as the input acceleration increases. Moreover, Fig. 3 shows that the magnitude factor decreases dramatically as the input acceleration increases further.

3. NONLINEAR COUPLING VIBRATION MODEL WITH 1DOF

3.1 Derivation of nonlinear coupling vibration model with 1DOF system

Here, we consider the relationship between flexural rigidity and out-of-plane deformation of the test tank when beam-type and oval-type vibration are coupled. Let us suppose that the entire tank vibrates, which represents beam-type vibration occurs, with large-amplitude vibration of the sidewall caused by oval-type vibration. This state implies that the occurrence of oval-type vibration produces a significant change in the cross-section shape of the tank. If the large amplitude caused by oval-type vibration is non-negligible relative to the thickness of the tank, it can be regarded as a large deflection, that is, out-of-plane deformation. This finding is a good hypothesis for the occurrence of geometric nonlinearity.

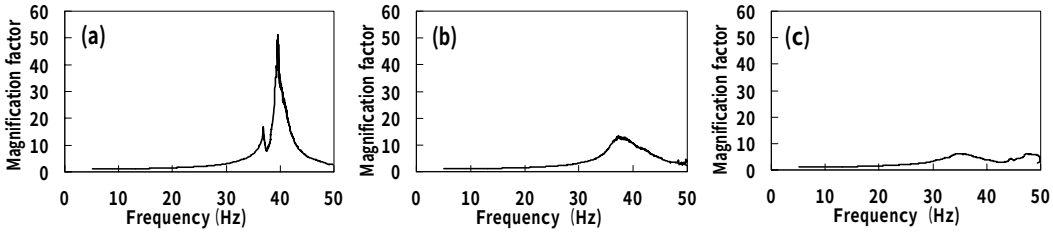

Figure 3: *Amplitude response curves under various input acceleration: (a) 0.09G, (b) 0.54G, (c) 1.16G.*

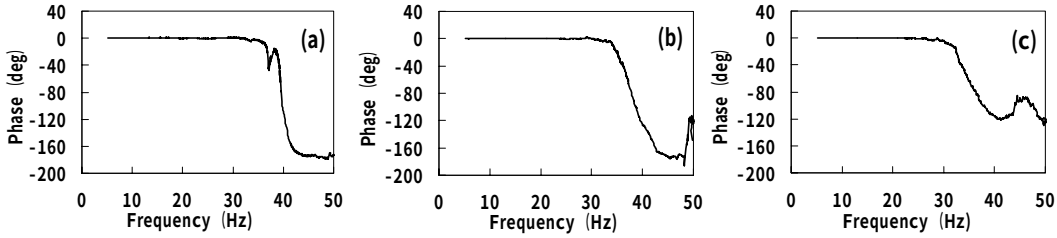

Figure 4: *Phase response curves under various input acceleration: (a) 0.09G, (b) 0.54G, (c) 1.16G.*

To verify this hypothesis, large-deformation analysis was performed by finite element method (FEM) and the relationship between sidewall out-of-plane deformation and flexural rigidity of the tank was assessed. First, as shown in Fig. 5(a), an FEM analysis model was made of the cylindrical test tank used in the vibration experiment. Next, as shown in Fig. 5(b), the model was given the oval-type vibration mode as imperfection shape and then it was defined as the test tank having the sidewall out-of-plane deformation caused by oval-type vibration. The amount of imperfection represents the amplitude of oval-type vibration, that is, its magnitude. Giving a static load to the entire FEM model, the flexural rigidity of the tank was calculated from the displacement magnitude at the top of the model. Varying the imperfection magnitude, the relationship between flexural rigidity and amplitude of oval-type vibration can be obtained. The analysis was carried out using NASTRAN code.

Figure 6 shows the relationship between the flexural rigidity of the tank and the amplitude of oval-type vibration. The vertical axis represents the ratio of flexural rigidity with the occurrence of oval-type vibration against that with no occurrence. This figure shows the analysis results with axial half wave number m=1 and various circumferential wave number n. Figure 6 reveals that flexural rigidity decreases as oval-type vibration increases. Especially in cases of a larger n value, the flexural rigidity decreases severely in excess of 10 mm of the amplitude. This feature is similar to that in other cases of various m (Maekawa et al., 2006). Consequently, it is clarified that the large amplitude of oval-type vibration causes the decrease in flexural rigidity of the tank. The geometric nonlinearity stated above is proposed to produce the nonlinear response of beam-type vibration.

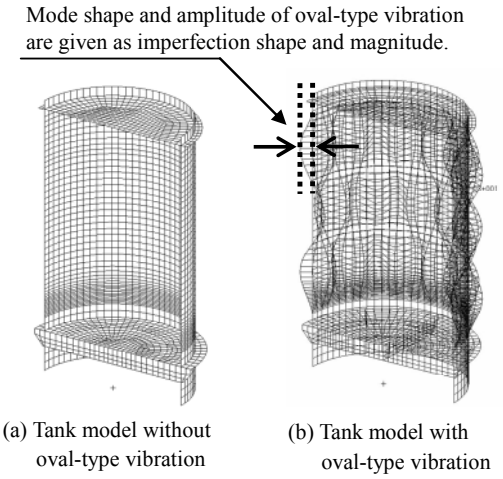

Figure 5: *Analytical model used to calculate the relationship between flexural rigidity of the tank and amplitude of oval-type vibration.*

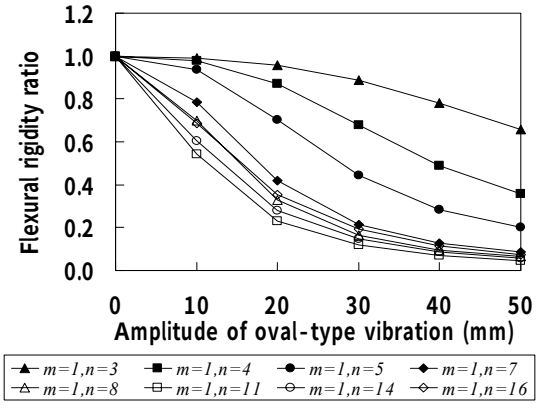

Figure 6: *Relationship between flexural rigidity of the tank and amplitude of oval-type vibration.*

Here, we create an equivalent nonlinear coupling vibration model with a 1DOF system based on the proposed hypothesis. First, the test tank is modeled as a beam of the 1DOF system. Then, the motion equation of the model is as follows:

$$m_0\ddot{x} + c\dot{x} + k_{NL}x = -m_0\alpha. \quad (1)$$

where m_0 is mass, x displacement, c damping coefficient, k_{NL} nonlinear spring constant depending on amplitude of oval-type vibration and α acceleration by external force such as earthquake motion. When the natural frequency of beam-type vibration having no amplitude of oval-type vibration is f_L, then k_{NL} of Eq. (1) corresponds to a linear spring constant, which is expressed by k_L. Then, the nonlinear spring constant k_{NL} with the occurrence of oval-type vibration is as follows:

$$k_{NL}/k_L = r(z). \quad (2)$$

where $r(z)$ represents a nonlinearity, the magnitude of which varies depending on amplitude z of oval-type vibration. In other words, it is the change rate of flexural rigidity depending on the amplitude of oval-type vibration. The relationship in Fig. 6 described above shows a typical example. Using Eq. (1) and (2) and defining ς as damping ratio, the following equation is obtained:

$$\ddot{x} + 4\pi\varsigma \cdot f_L\dot{x} + (2\pi f_L)\cdot r(z)\cdot x = -\alpha. \quad (3)$$

Equation (3) represents the motion equation of the equivalent nonlinear coupling vibration model with 1DOF system.

3.2 Numerical analysis by equivalent nonlinear coupling vibration model with 1DOF system

Here, using the equivalent nonlinear coupling vibration model with 1DOF system, we demonstrate that the influence of oval-type vibration on beam-type vibration causes the shift in resonance frequency to the lower frequency region. Table 2 shows the analysis conditions. m represents the axial half wave number and n the circumferential wave number. f indicates natural frequency and ς damping ratio. The data in Table 2 was obtained by eigenvalue analysis of the FEM model. In the numerical analysis, each oval-type vibration shown in Table 2 is assumed to have occurred because the purpose of the analysis is to verify the relationship between the characteristics of beam-type vibration and the out-of-plane deformation generated by oval-type vibration. In addition, the constant damping ratio as shown in Table 2 is used on the assumption that there is no influence of oval-type vibration to change the damping ratio. The relationship as shown in Fig. 6 is used as $r(z)$ of Eq. (3). Figure 6 is an analytical case of m = 1 and additional analysis has been conducted for the case of m = 2 and 3 (Maekawa et al., 2006).

Figure 7 shows the relationship between the declining rate of resonance point of beam-type vibration and the amplitude of oval-type vibration. Moreover, analytical and experimental results are compared. The vertical axis represents the ratio of resonance frequency with oval-type vibration against the natural frequency without it. The analytical results show that the resonance frequency of beam-type vibration becomes lower as the amplitude of oval-type vibration increases. In general, the declining rate is similar to that in the experiment. Especially, the pattern in the case of m = 1 is in good agreement with that in the experiment. Therefore, it is concluded that the proposed 1DOF system model can explain the shift phenomenon in the resonance frequency of beam-type vibration under large excitation. In other words, the coupling between beam-type and oval-type vibration changes the flexural rigidity of the beam-type vibration. As a result, the beam-type vibration causes the nonlinear vibration response.

Case	Oval-type vibration			Beam-type vibration			
	m	n	f(Hz)	m	n	f(Hz)	ς (%)
A	1	8	25.0	1	1	45.0	1
B	1	12	52.4	1	1	45.0	1
C	1	14	78.5	1	1	45.0	1
D	2	14	83.8	1	1	45.0	1
E	3	14	95.7	1	1	45.0	1
F	1	12	52.4	1	1	45.0	10

Table 2: *Analytical conditions using 1DOF model.*

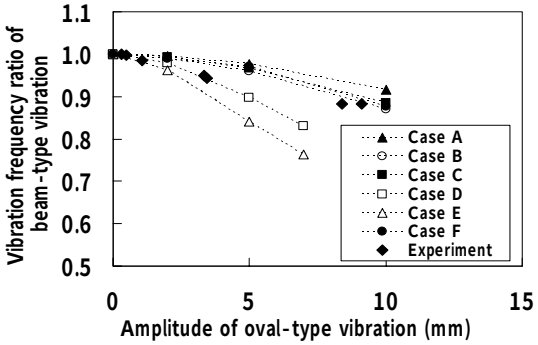

Figure 7: *Analytical results by 1DOF model.*

4. NUMERICAL ANALYSIS BY NONLINEAR FINITE ELEMENT METHOD USING EXPLICIT METHOD

4.1 Analytical method and model

This section describes the nonlinear FEM proposed and conducted to clearly show that the oval-type vibration influences the characteristics of the beam-type vibration.

The following points are important for highly accurate simulation of the oval-type vibration:

- Three-dimensional modeling.
- Coupling analysis between fluid and structure because oval-type vibration produces the coupling vibration system consisting of the tank structure and the contained water.
- Large-deformation analysis because of its highly accurate simulation of large-amplitude motion by oval-type vibration.
- Time-history analysis.

Considering the above, a time-history analysis utilizing FEM and taking into account coupling analysis between fluid and structure and large-deformation analysis was developed. The structural part of the analytical model had the shell element for geometric nonlinearity. Belytschko-Lin-Tsay shell element (Belytschko et al., 1984) was used in this analysis. The fluid part had the solid element following Euler's equation. These elements were also needed for three-dimensional modeling. The arbitrary Lagrangian-Eulerian (ALE) method was adopted for the coupling analysis between fluid and structure. Explicit time integration method using centered difference was adopted for the time-history analysis considering stability of solution. The general code LS-DYNA was used in actual analysis. It was previously reported that this method had the potential to simulate oval-type vibration with a high degree of accuracy (Maekawa et al., 2007).

Figure 8 shows the analytical model. The total number of nodes is 30023. The number of shell elements in the structural part is 7144 and the number of solid elements in the fluid part is 25800. The outer lip of the tank, etc. was left out for rationalization of modeling. The material constants are summarized in Table 3. In this table, E represents Young's modulus, υ Poisson's ratio, ρ density and K bulk modulus. Sinusoidal wave frequency sweep was performed in this analysis as in the case of the experiment. The sweep rate was 0.2 Hz/s as in the experiment and the excitation direction was horizontal. The input acceleration was 0.09 and 1.16 G. The amplitude response curve was calculated between response displacement at the top of the analytical model and input displacement.

Figure 9 shows analytical results. Deformation of the tank wall demonstrates that the method can accurately simulate behavior of oval-type vibration with large amplitude.

	E (MPa)	ν	ρ (kg/m^3)	K (MPa)
Al alloy (tank body)	69420	0.33	2680	–
Steel (platform/flanges)	203000	0.3	7800	–
Polycarbonate (top plate)	1960	0.3	1190	–
Water (in the tank)	–	–	1000	2200

Table 3: *Material constants used in FEM analysis.*

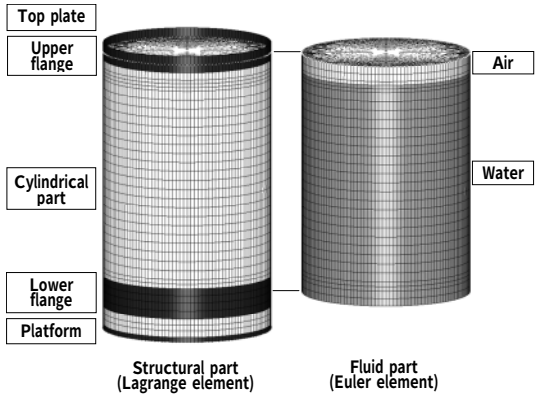

Figure 8: *Analytical model for nonlinear FEM.*

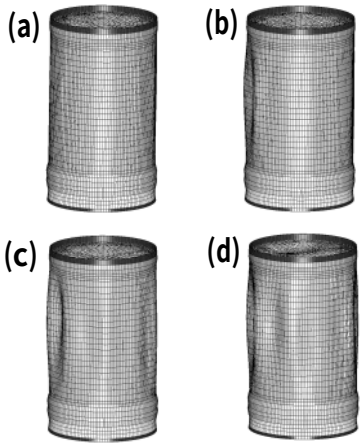

Figure 9: *Analytical deformation views (scale factor: 10) of the model at excitation frequency: (a) 36Hz, (b) 37Hz, (c) 38Hz, (d) 39Hz.*

4.2 Comparison between analytical and experimental results

Figure 10 shows the relationship between input acceleration and resonance frequency. The natural frequency of the test tank used in the experiment is 40.23 Hz and that of the analytical model is 41.04 Hz. From this difference, the vertical axis of Fig. 10 is represented by the ratio of resonance frequency against these natural frequencies. The analytical

results are in good agreement with the experimental results. Figure 11 shows the relationship between input acceleration and magnification factor. The analytical results in the case of input acceleration of 1.16 G agree very well with the experimental results. The value in the case of 0.09 G differs slightly from that in the experimental. However, the Q factor is so large in such small excitation and the resonance curve is so sharp that the result values often fluctuate due to a bit of error in the analytical conditions.

From the items discussed above, it can be concluded that the proposed nonlinear dynamic analysis using FEM can simulate, with a high degree of accuracy, the nonlinear vibration response of the test tank as obtained in the experiment. This analytical result shows that the oval-type vibration increases and is coupled with the beam-type vibration and consequently influences the characteristics of the beam-type vibration. In other words, the generating mechanism of the nonlinear response of the beam-type vibration is proposed.

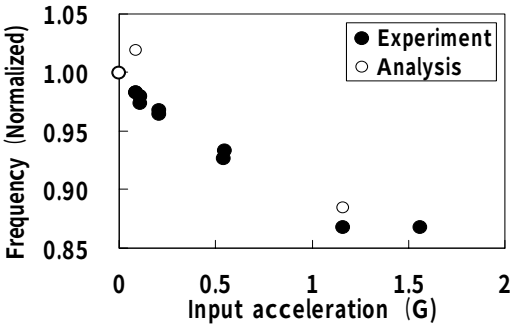

Figure 10: *Relationship between input acceleration and resonance frequency.*

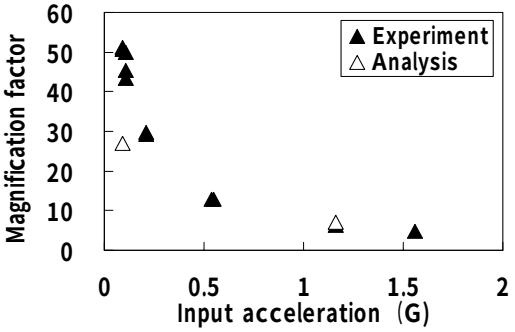

Figure 11: *Relationship between input acceleration and magnification factor.*

5. CONCLUSION

It was clarified experimentally that the nonlinear vibration response of a cylindrical water storage tank occurred upon extreme excitation. Nonlinear behavior showed a shift in resonance frequency to a lower region and a decrease in magnification factor. A coupling vibration model with 1DOF system and nonlinear FEM taking into account large-deformation analysis and coupling vibration analysis between fluid and structure were proposed. The analytical results demonstrated that the nonlinear vibration response was caused by the coupling effect with oval-type vibration. The proposed nonlinear FEM analysis method comprises the ALE method as the coupling analysis, large-deformation analysis using nonlinear shell element and time-history analysis by explicit method. Comparison with the experimental results indicated that the proposed FEM method can simulate the nonlinear vibration behavior with a high degree of accuracy.

6. REFERENCES

Amabili, M., 2000, Eigenvalue problems for vibrating structures coupled with quiescent fluids with free surface. *Journal of Sound and Vibration*, **231-1**:79-97.

Belytschko, T. et al., 1984, Explicit Algorithms for the Nonlinear Dynamics of Shells, *Computer Methods in Applied Mechanics and Engineering*, **42**:225-251.

Chiba, M. et al., 1986, Dynamic stability of liquid-filled cylindrical shell under horizontal excitation, Part I: Experiment. *Journal of Sound and Vibration*, **104-2**:301-319.

Fujita, K. and Saito, A., 2003, Free vibration and seismic response analysis of a liquid storage thin cylindrical shell with unaxisymmetric attached mass and stiffness. *Proceedings of ASME PVP*, **466**:243-252.

Maekawa, A. et al., 2006, Nonlinear vibration response of a cylindrical water storage tank caused by coupling effect between beam-type vibration and oval-type vibration: Part 2–Simulation. *Proceedings of ASME PVP*, **PVP2006-ICPVT-11-93263**:1-8.

Maekawa, A. et al., 2007, Nonlinear vibration behavior of a cylindrical water storage tank and numerical analysis by finite element method. *Proceedings of 12th Asia Pacific Vibration Conference*.